2.3 Quantum diffusive transport: weak localisation

In the preceding section 2.2 we discussed classical diffusive transport, i.e. in the limit where the phase coherence length l_φ (which we, as usual, loosely "mix" with the inelastic length l_i) is very much smaller than the size of the system. In this section we will discuss the opposite limit, defined by

$$\lambda_F \, , \, l_e << L \, , \, l_{i,\varphi}$$

In chapter 1 we discussed the fundamentally different nature of inelastic (or phase breaking) and elastic (non-phase breaking) scattering. The preservation of the phase as occurring in elastic scattering will maintain quantum interference, which will be shown to lead to marked effects in the conductance in this regime. Evidently to experimentally enter this regime we should bring the system at low temperatures to suppress phase-breaking influences like phonons.

The phenomenon we will concentrate on goes under the name of *weak localisation* (WL). Basically it results from the (quantum induced) *enhanced probability* for electrons experiencing many elastic scatterings to *return to their initial position*. This leads to a tendency for electrons to "stay where they are", i.c. some kind of electron localisation, resulting in a reduction of the conductance of the system.

2.3.a. *A simple introduction to the theory of quantum corrections to the conductance: Weak Localisation effect*

In deriving the Drude expression for the conductivity, eq. (2.3), a fundamental assumption is that each scattering event fully destroys all information on the initial velocity (size and direction) of the particle. In quantum terms this also implies that the phase correlation is completely suppressed during such event. If however, in contrast, the phase of the electron is (partially) preserved during scattering, this will affect the diffusion coefficient and so the conductance employing the Einstein relation eq. (2.8). From this equation, which contains the diffusion coefficient D given by the Kubo expression (2.10), it is immediately clear that conservation of the phase will introduce a correlation between the velocities for times *beyond the elastic scattering time* τ_e *and up to the phase-coherence time* τ_φ.

A fundamentally correct derivation of weak localisation requires a rather involved mathematical approach based on so-called diagrammatic techniques, which is well beyond the scope of our introductory text. We will use an approach employing "ray or geometric optics", augmented by the phase per raytrace, called the *Feynman path* method. Figure 2.8 shows the basic ingredients of this approach. The transport of an electron from an initial position 1 to a final position 2 is described as the transmission of an electron wave from 1 to 2 through the diffusive medium. This implies that the electron wave, starting at position 1, will become distributed over a number of *partial waves* ψ_j, each traversing the system along a different path p_j while experiencing many *elastic* scattering events before ultimately arriving at 2.

It should be noted that, to allow the use of the semi-classical Feynman paths to evaluate the total transmission probability, we implicitly assume that the electron really can follow a well-defined path, i.e. it should not be scattered too strongly on its characteristic length

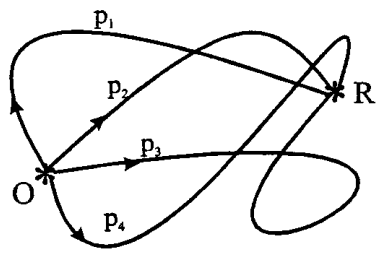

Figure 2.8. Electron waves travelling through a disordered medium containing elastic scatterers. The wave of a single electron at position O is distributed over a number of partial waves ψ_j, each following a well-defined path p_j, arriving at position R with a transmission coefficient t_j. Note that the phase φ_j on arriving at position R depends on the path length thus differing for each individual path.

scale, λ_F. As discussed immediately following eq. (2.5), violating this condition will lead to strong localisation, a phenomenon requiring a completely different description. To calculate the total quantum mechanical probability for the electron to travel from *O=>R* we have to evaluate the *vector sum* of all the partial waves arriving at *R*, i.e. including the *phases* φ_j of all the partial waves as acquired while following their individual paths. Figure 2.9 shows a scattering medium with a number of scatterers *, denoted by 0, 1, 2, 3, ...The electron wave is taken to start at position 0. We can distinguish between two different sets or ensembles of paths. The first set just connects two random positions, e.g. 0 and 7. Paths like {0,1,7}, {0,4,2,7}, {0,5,4,3,2,7} etc. all contribute to the total amplitude of the wave at 7, which then is given by

$$\Psi(7) = \sum_j \psi_j = \sum_j t_j \exp(i\varphi_j) \qquad (2.17)$$

Note that such a sum also contains contributions from multiple scattering, e.g. a path such as {0,4,2,4,2,7} is included, and so evaluating it will be a matter of tedious and accurate bookkeeping!

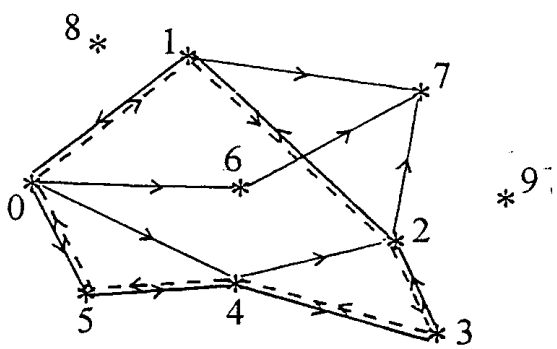

Figure 2.9. An electron wave starting at position 0, with its partial waves travelling along various paths. The solid lines show paths leading from 0 to (a randomly chosen final) position 7. The dashed sequence of lines forms a path that allows the electron to return to its starting position 0.

Formally, from eq. (2.17) we straightforwardly can write down the total probability for the wave at (say) position 7, as

$$P(7) \equiv |\Psi(7)|^2 = \sum_j t_j^2 + \sum_{j \neq k} t_j t_k \cos(\varphi_j - \varphi_k) \qquad (2.18)$$

Now we assume that *many different paths* contribute to the total amplitude. In the second term of eq. (2.18), containing the cross-product terms, the *random distribution* of the phases φ_j for all the paths p_i yields on average as many positive and negative contributions, thus reducing its sum to a small value. So, the total probability for forward transfer between two randomly chosen positions (0 and 7 in our case) approximately is just the sum of the probabilities of the individual partial waves.

$$P_{fwrd} \approx \sum_j t_j^2 \qquad (2.19)$$

Next we pose the question what happens if we take the initial and final position in space to be *the same*. This implies that we want to know what probability is associated with *returning* to the initial point. In figure 2.9 paths like e.g. {0,1,7,6,0} and {0,5,4,0} are typical examples, taken for the starting position 0. Let us look in a little more detail to the various trajectories involved in the total return probability. Concentrating first on randomly chosen *different* paths, it is evident that the same argument holds concerning the phases as given before for the different points in space and thus the total probability resulting from these trajectories is again the simple sum of the partial probabilities (eq. (2.19)).

However, in addition to these randomly chosen paths we also have to include a particular type of *complementary* trajectories. More specifically a typical example in figure 2.9 is {0,1,2,3,4,5,0} and {0,5,4,3,2,1,0}, i.e. the first is the *time-reversed* version of the second (and vice-versa). These time-reversed twins of course are not independent. In particular the identical length of the two paths implies that the phase-differences acquired during travel will be exactly the same. In addition the symmetry of elastic scattering events dictates that also the amplitude of the two partial waves will be the same.

Write j_{j+} for the amplitude of the wave along path p_j taken in one particular direction (say, clockwise), and t_{j-} for the arriving amplitude after traversing the path in the opposite, counter-clockwise direction. For the total contribution of this path to the return probability we thus find

$$P_j(0 \rightarrow 0) = t_{j+}^2 + t_{j-}^2 + t_{j+} t_{j-} \cos(\varphi_j - \varphi j + t_{j-} t_{j+} \cos(\varphi_j - \varphi_j) = 4t_j^2 \quad (2.20a)$$

as $t_{j+} = t_{j-} = t_j$ from the symmetry argument. For the results after summing the contributions of all paths we thus find

$$P_{return} \equiv P(0 \rightarrow 0) = \sum_j P_j(0 \rightarrow 0) = 4 \sum_j t_j^2 \qquad (2.20b)$$

One factor of 2 results from the fact that we simply have summed over two trajectories per entry j: for each path denoted by a single j also the complement was taken in the sum. However then we are still left with a second factor of 2. This factor is the direct consequence of the coherent, in-phase addition of time-reversed paths.

So we conclude that the *phase-coherent summation of time-reversed trajectories in a diffusive medium leads to an increased probability for electrons to return to their initial position.* This is commonly referred to as *coherent back scattering*. It implies that electrons indeed tend to remain at their initial site, an effect which leads to a reduction of the conductance (and an increase of the resistance) of the system, denoted as *Weak Localisation (WL).*

Before providing a more quantitative estimation of the strength of weak localisation in the conductance we first want to demonstrate a quite remarkable effect associated with the directions of the electron waves involved in this quantum coherent return phenomenon. Figure 2.10 shows two specific scatterers 1 and 2, with a plane electron wave incident on the two from the left. The wave, with the incoming plane wave front at A indicated by the dashed line, is (partially) scattered directly at each scatterer and returned, but in addition it is (partially) scattered to the other scatterer at a distance Δr_{12}, followed by returning to the left. To calculate the total leftwards outgoing wave we have to (coherently) sum the individual contributions, including the phases, and see what condition is required to recover a plane wave front at B and C, denoted by the dashed lines. Now consider the two parallel rays R1 (top) and R2 (bottom) of the incoming beam. R1 is scattered from 2 to 1 and we assume it to leave 1 at an angle δ relative to the incoming direction. The lower ray R2 follows the path 1 to 2 (i.e. reverse as compared to R1) and we look at the ray leaving 2 at the same angle δ. Note that the figure also shows the rays leaving at the complementary angle $-\delta$.
The difference in pathlength, $\Delta l_{12}(\delta)$, between the two rays that leave 2 and 1 immediately follows from the geometry, yielding

$$\Delta l_{12}(\delta) = a - a' = \Delta r_{12}(\cos(\theta) - \cos(\theta')) \qquad (2.21a)$$

with $\theta' = \theta + \delta$ (and $\theta'' - \delta$ for the complement) is the angle between Δr_{12} and the direction

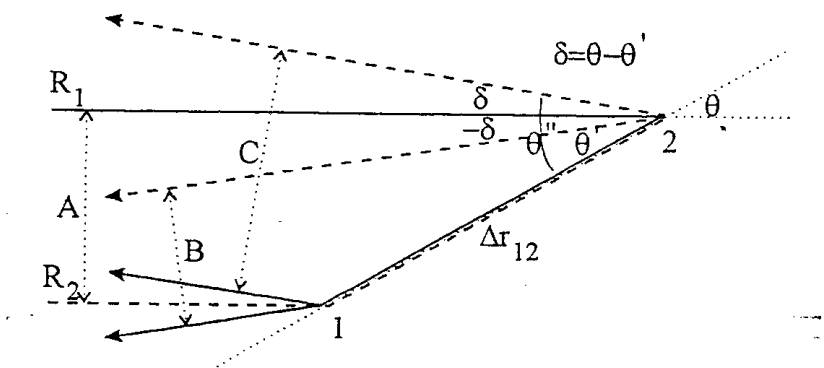

Figure 2.10. Coherent back-scattering of a plane electron wave at A incident on two elastic scatterers 1 and 2. At B a wave front leaving the scatterers at an angle $-\delta$ relative to the incoming beam is shown; similarly a wave front leaving at $+\delta$ is indicated at C.

of the incoming wave (see figure 2.10). Assuming δ to be small (see below) we find for the associated difference in phase

$$\Delta\varphi_{12}(\pm\delta) = 2\pi\frac{\Delta l_{12}(\pm\delta)}{\lambda_F} \approx 2\pi\frac{\Delta r_{12}}{\lambda_F}\{-\frac{1}{2}\delta^2 cos(\theta) \pm \delta\, sin(\theta)\} \qquad (2.21b)$$

For the *total* outgoing wave we have to sum the + and - terms and so the contributions due to the sin(θ) term cancel, so we only have to consider the cosine term. The contributions of the two rays only add constructively if they differ in phase by no more than ~π/2. As the alignment of the two scatterers is completely random, we now have to average over all possible directions of Δr_{12} relative to the incoming beam, i.e. with the angle θ covering the range $-\pi/2<\theta<\pi/2$. This yields for the average over angle

$$< \Delta r_{12}\, cos(\theta) > \approx \Delta r_{12}/2 \approx l_e/2 \qquad (2.22)$$

the last equality resulting from the fact that we take the two scatterers at their minimum average separation $\Delta r_{12} \sim l_e$. Combining eq. (2.22) with eq. (2.21b) and including the limit $<\Delta\varphi_{12}> \leq \pi/2$ we find the following maximum angle δ_{max} for the *reflected outgoing wave* relative to the incoming wave

$$\delta_{max} \approx \sqrt{\lambda_F / l_e} \qquad (2.23)$$

As discussed previously we limit ourselves to the case that the electron can travel freely at least over a number of wavelengths or $\lambda_F << l_e$, which implies that $\delta_{max} << 1$. So we have to conclude that the reflected wave only has an appreciable intensity within a (2D or 3D) cone with a (small) top-angle $2\delta_{max}$ relative to the direction of the incoming beam. This underlines that indeed the wave is truly *back-reflected* in a *coherent* way.

Now we are in the position to calculate quantitatively the effect of weak localisation on the conductance of the system. For the sake of simplicity we will limit the discussion to the 2D case. We employ the celebrated Einstein relation, eq. (2.8), for the conductivity and see how the coherent backreflection reduces the diffusion coefficient by an amount ΔD.
Using the Kubo expression (2.10) for D as the velocity-velocity correlation,

$$D = \int_0^\infty < \vec{v}_x(t)\vec{v}_x(0) > dt$$

we evaluate the correction resulting from the increased correlation due to the coherent backscattering, with $|v_x(t)| \sim |v_x(0)| \sim v_F$. The (negative) contribution to D thus can be written as

$$\Delta D \approx - < v_F v_F * \delta_{max}^2 * P_{return}(\Delta S(\vec{r} = \vec{0})) >_{direction} \qquad (2.24)$$

with $<....>_{direction}$ denoting the averaging over all (2D) directions of the incoming beam, as usual for the calculation of the diffusion coefficient. It leads to the $1/d$-factor, with d denoting the dimensionality of the problem (see also eq. (2.9)). The maximum angle δ_{max} is included squared as we are calculating the return *probability*. From our semi-classical ray-optics picture $P_{return}(\Delta S(r=0))$ is the (classical) probability for the particle, starting at

a certain position r=0, to return to within an area of size ΔS around this initial position, and within a time scale that is relevant for the problem at hand; note that this "origin" can be taken completely arbitrarily. This probability integrated over all times can thus be written

$$P_{return}(\Delta S(\vec{r}=\vec{0})) = \Delta S * C_{return} = \Delta S \int_0^\infty C(\vec{0},t)dt \equiv \Delta S \frac{1}{n_0}\int_0^\infty n(\vec{0},t)dt \qquad (2.25)$$

with $n(0,t)$ given by expression (2.12), i.e. representing the probability to return to the initial position at a certain time t. From (2.12) we immediate find for the 2D case

$$n_{2D}(\vec{0},t) \equiv n_0 C_{2D}(\vec{0},t) = \frac{n_0}{4\pi D t} \qquad (2.26)$$

Before proceeding by evaluating the integral of (2.25) we have to include two more terms to it, based on the relevant time scales in the problem. First, we have to realise that electrons traveling for times *shorter* than the elastic scattering time $\tau_e = l_e/v_F$ will not be able to return what so ever, and so they will not contribute to the backscattering. This might be accounted for by changing the lower limit to the integral from 0 to τ_e, but to allow for the statistical nature of this aspects it is covered by multiplying $C(0,t)$ by the factor $(1-\exp(-t/\tau_e))$. Secondly, there is also an upper bound to the integral: by the time the wave loses its phase coherence it no longer can contribute to *coherent* backscattering and so we should limit the integral to times smaller than the phase breaking time τ_φ. Again by accounting for the statistical nature it is incorporated by multiplying by the factor $\exp(-t/\tau_\varphi)$.

The last term to be defined in eq. (2.25) is the return area ΔS. From the discussion around the figures 2.9 and 2.10 it is clear that we can not define "a return" any better than given by the average distance between elastic scatterers $\Delta r_{12} \sim l_e$, and so we immediately find (in 2D) for the typical return area $\Delta S \sim l_e^2$.

Introducing the three factors into eq. (2.25) and including also eq. (2.26) we find

$$\Delta D_{2D} \approx -\frac{l_e^2 v_F^2 \delta_{max}}{2*4\pi D}\int_0^\infty \frac{1}{t} exp(-\frac{t}{\tau_\varphi})(1-exp(-\frac{t}{\tau_e}))dt \qquad (2.27)$$

The time-integral yields $\ln(1+\tau_\varphi/\tau_e)$, which equals $\sim\ln(\tau_\varphi/\tau_e)$ if the phase breaking time is much larger than the elastic time.

Thus the final expression for the weak localisation correction to the conductance reads

$$\Delta\sigma_{2D} = e^2 \rho_{2D} \Delta D_{2D} \approx -\frac{1}{4\pi}\frac{2e^2}{h} ln(\frac{\tau_\varphi}{\tau_e}) \qquad (2.28)$$

It demonstrates two important properties. First, its size is of the order of the conductance quantum e^2/h. Secondly it is only weakly dependent on the ratio of the phase breaking length and the elastic length, once this ratio is >>1.

Equation (2.28) is for the 2D case; similar expressions can be obtained for the 1D and 3D case. One finds that the effect strongly increases at a reduction of the dimensionality, i.e. it is largest in 1D.

It is also noteworthy to see that the dimensionality for weak localisation is governed by the phase breaking length l_φ in comparison to the size of the system.

Before proceeding to discuss some experimental results that demonstrate this quantum interference effect in the diffusive regime we first have to consider how one would be able to determine it: if the WL only reduces the conductivity by a small fraction we need a way to distinguish between the classical conductance (eq. (2.7a)) and the correction due to WL (eq. (2.28)). To this purpose we consider the effect of an applied magnetic field on the WL effect, and we will find that for sufficiently large fields the correction $\Delta_{WL}\sigma$ from eq. (2.28) becomes suppressed. This allows us to distinguish between the classical and the WL contribution.

Applying a magnetic field to an electron travelling at a velocity v_F results in two effects:

= Classically it will bend the path of the electron due to the Lorentz force, leading to the formation of the circular cyclotron orbits; we have discussed this in chapter 1, eqs. (1.8). The important question we have to pose is how this curvature affects the WL correction, i.e. what effect does it have on a trajectory and its time-reversed complement (see again figure 2.9). Evidently the field-induced curvature affects the precise shape of the trajectories. In particular, the two time-reversed trajectories will become increasingly dissimilar for increasing field strength. However, at the small fields required to affect the WL (see below) the effect due to the curvature turns out to be negligible.

= Quantum mechanically the magnetic field affects the canonical momentum p via the vector potential A defined by the magnetic field as $\vec{B} = \vec{\nabla} \wedge \vec{A}$. From introductory quantum mechanics we know that for a charge q=-e

$$\vec{p} = \hbar\vec{k} = m\vec{v} + q\vec{A} = m\vec{v} - e\vec{A} \tag{2.29}$$

which implies that the wavevector k becomes B-dependent. The electron travelling at the Fermi energy from position 1 to 2 along a path defined by $\vec{l}$ acquires a phase

$$\Delta\varphi_{1\to 2} = \int_1^2 \vec{k}\cdot d\vec{l} = 2\pi\frac{m}{h}\int_1^2 \vec{v}_F \cdot d\vec{l} - 2\pi\frac{e}{h}\int_1^2 \vec{A}\cdot d\vec{l} = \Delta_v\varphi_{1\to 2} + \Delta_A\varphi_{1\to 2} \tag{2.30}$$

Note that the phase acquired following the trajectory is affected by the magnetic field via the second term of eq. (2.30), i.e. via the *vector potential.* We will return to this aspect in more detail in chapter 5.

Now let us concentrate on a typical WL trajectory, i.e. a time-reversed pair that (approximately) returns to its initial position after a number of elastic scatterings (figure 2.11). The resulting closed trajectory implies that in the expression (2.30) for the phase the integral should be interpreted as a loop integral enclosing the area S. For the phase this yields

$$\Delta_{1\to 2}\varphi = k_F L - 2\pi\frac{e}{h}\oint \vec{A}\cdot d\vec{l} = k_F L - 2\pi\frac{e}{h}\iint \vec{B}\cdot d\vec{S} = k_F L - 2\pi\frac{e}{h}\Phi \tag{2.31}$$

with Φ denoting the *flux B.S penetrating the area enclose by the closed trajectory*. The quantity h/e is called the (single charge) *flux quantum*, written as Φ_0=h/e. Now take the two time-reversed trajectories. Encirculating it clockwise will yield

$$\Delta_{clws}\varphi = k_F L - 2\pi\frac{\Phi}{\Phi_0} \tag{2.32a}$$

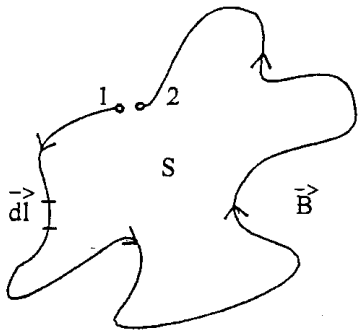

Figure 2.11. A typical trajectory that contributes to weak localisation, allowing an electron to leave from 1 and, after a number of elastic scattering events, returning to a position 2, or vice versa going from 2 to 1; 1 and 2 are separated by less than an elastic length l_e. The trajectory encloses an area indicated by S.

while traversing it in the opposite (i.e. counter clockwise) direction yields

$$\Delta_{cclws}\varphi = k_F L + 2\pi\frac{\Phi}{\Phi_0} \qquad (2.32b)$$

Note that the zero-field term $k_F L$ is (evidently) independent of the direction of travel. For the *difference* in phases acquired in travelling clockwise and counter clockwise along the time-reversed paths we thus find

$$\Delta\varphi = \Delta\varphi(B) = (2\pi - (-2\pi))\frac{\Phi}{\Phi_0} = 4\pi\frac{\Phi}{\Phi_0} = 4\pi\frac{BS}{\Phi_0} \qquad (2.33)$$

Note that the magnetic field enforces the two time-reversed trajectories to become dissimilar as far as their phases are concerned. Stated differently, a magnetic field leads to *time-reversal symmetry breaking*, a very general quantum phenomenon associated with the application of magnetic fields.

As we have discussed in relation to eq. (2.20) at zero B-field the fully *in-phase* coherent summation of the waves of the two time-reversed paths resulted in the factor-of-2 increase of the probability for back scattering. This implies that the phase-shift (2.33) induced by the field will *reduce* this sum following $\cos(\Delta\varphi(B))$, *i.e. the magnetic field indeed affects the contribution to the weak localisation.* In particular, at such a field that this shift amounts to $\sim\pi/2$ the (zero field) constructively interfering contribution to WL (from that particular path) at a certain B-field will turn into a destructively interfering contribution, and so it will become suppressed.
Now we have to realise that the total WL effect results from contributions from a large ensemble of individual (pairs of time-reversed) trajectories, each of different shape and size and so enclosed areas S_j. At a given field the phase shift depends (linearly) on the area S_j associated with each particular trajectory p_j. More specifically, for the whole set of trajectories the longer ones, which most likely (but not necessarily!) will also enclose the larger areas S, will acquire a larger phase shift than the shorter ones. The longest paths which can contribute to WL are those with a size of approximately the phase coherence

length, i.e. $L_{max}<\sim l_\varphi$, with an associated enclosed area $S_{l_\varphi} \approx \pi(l_\varphi / 2\pi)^2$. These will yield the largest phase shift at a given field. So, as a consequence, and based on eq. (2.33), weak localisation will start to become suppressed whenever

$$\Delta\varphi \approx \frac{\pi}{2} \approx \frac{2\pi}{\Phi_0} S_{l_\varphi} B_c = \frac{2\pi}{\Phi_0} \pi (\frac{l_\varphi}{2\pi})^2 B_c \qquad (2.34a)$$

From this a characteristic field B_c can be defined where the suppression starts to become effective

$$B_c \sim \frac{\Phi_0}{l_\varphi^2} = \frac{h}{e l_\varphi^2} \qquad (2.34b)$$

So, in conclusion, *weak localisation can be suppressed by applying a magnetic field such that the zero-field time-reversed trajectories become dissimilar in acquired phase due to time-reversal symmetry breaking*. This suppression of WL provides a way to study the effect experimentally.

2.3.b. *Experiments on Weak Localisation*

In the following part we discus two experiments showing weak localisation in the conductance, one on a semiconductor system and one on a metal. In order to demonstrate the very general nature of coherent backscattering in disordered system we show a third experiment which is not associated with electrons but employs optical waves.

1. Weak localisation in two-dimensional electron gas in a Si-MOSFET.
We first concentrate on the effect in a 2-dimensional electron gas in a semiconductor structure. (D.J. Bishop et.al., Phys. Rev. B26, 773-779 (1982)). The 2DEG is formed at the interface of a Si-MOSFET, the gate of which allows the electron density to be controlled; in this way the diffusion constant can be varied via the elastic mean free path and the Fermi velocity (see eq. 2.9). Figure 2.11 shows one of the results obtained in the experiment (noisy curve, "overlapped" by the solid curve b; the (fitting) curves a, b and c result from a full theoretical treatment). It is obtained at T=100 mK and an electron density n_e~4.5*10^{16} m^{-2}. Note the characteristic field scale for reaching a "field-independent" value B_c~ a few times 0.1T (note: 1 kG=0.1T).

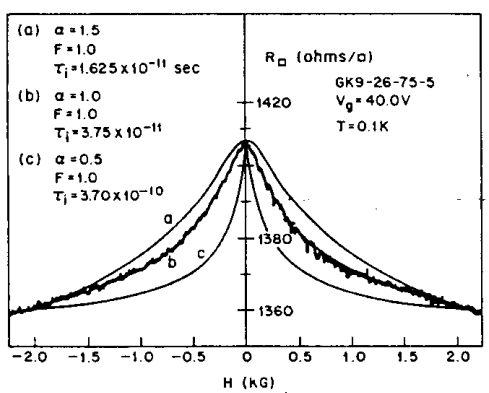

Figure 2.12. Reduction of the resistance with magnetic field, due to suppression of the weak localisation, in a 2D electron system at the Si-SiOx interface. The "noisy curve" is the actual experimental data. The smooth curves a, b and c represent different curves resulting from a fit to the theory.

Problem: Rewrite the resistance contribution due to WL in figure 2.12 in a change in the conductance; is the value thus found in reasonable agreement with eq. (2.28) assuming the logarithmic term to be of order unity?
Problem: Take from the original paper of Bishop et.al. the mobility. Evaluate the elastic mean free path from the electron density and the mobility. Evaluate also the phase coherence length from the characteristic field scale of fig. 2.12, using eq. (2.34b). Is the assumption of the near-unity value of the ln-term allowed?

2. Weak localisation in a thin metallic Mg film.
In this magnetoresistance experiment Bergmann (Phys. Rev. B25, 2937-2939 (1981); see also Physics Reports 107, 1-58 (1984): the figures are taken from this last paper, i.e. their figures 2.11. and 2.12) investigates the magnetic field dependence of the conductance of a very thin Mg film evaporated onto a crystalline quartz substrate. Homogeneous films with thicknesses varying between 7 and 12 nm were obtained by performing the evaporation with the substrate held at ~ 5K. The data points, shown in figure 2.13a, are taken at five different temperatures between 4.5 and 20K. The magnetic field for each temperature is indicated next to each individual experimental curve; it varies for the range of temperatures taken in this experiment. This change of characteristic field scale is

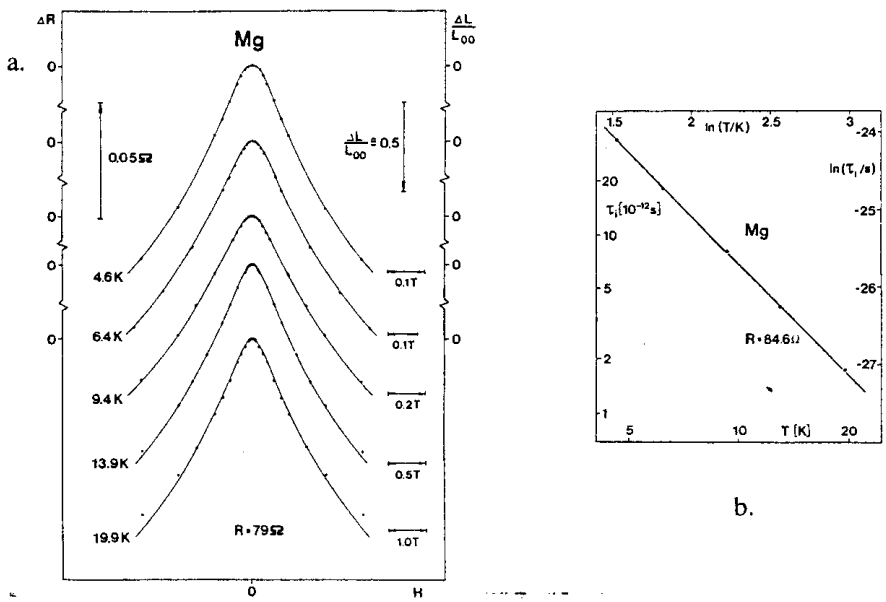

Figure 2.13. Weak localisation in a thin Mg film. Panel a. shows the experimental results obtained at five different temperatures between 4.6 and 19.9 K. The resistance in an applied magnetic field shows the characteristic behaviour of weak localisation, with a (temperature dependent) suppression field. In panel b. the phase breaking time is shown as deduced from the measurements.

accordance with the decrease of the phase breaking length with increasing temperature (eq. 2.34b). The full curves are fits to a full theoretical treatment of the WL problem; note the very good agreement obtained in this fit! From these results it is rather straightforward to evaluate the temperature dependence of the phase breaking time; this is shown in figure 2.13b.

Problem: Determine the dimensionality of this WL experiment. For this to do, remind yourself on which length scales are relevant. Take the needed values from the Phys. Rev paper of Bergmann.

3. Coherent backscattering in optics: the narrow coherent cone.-
The third experiment we want to discus seems to be of a completely different nature. In the preceding discussion we have concentrated on *electron* waves in diffusive systems. However, from the whole line of reasoning it is completely self-evident that the whole line of reasoning that leads to WL should hold for *any type of waves* in a diffusive medium! So it is anticipated that also mechanical waves (e.g. in acoustics) or electromagnetic waves should show the same phenomenon, with the (important!) exception that a magnetic field will not be able to break the time-reversal symmetry in these cases. This missing control mechanism (or "experimental knob") thus demands a different approach in order to investigate the phenomenon, in order to separate the WL contribution from the much larger "classical" background. This can be done by employing the aspect of coherent backscattering into a narrow cone as discussed before (see figure 2.10). We found the important result that a beam incident onto the diffusive medium shows an increase probability of being backreflected, preferentially within a cone

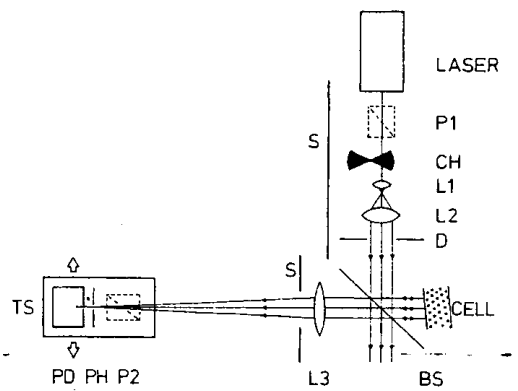

Figure 2.14. Schematic diagram of the optical set-up to study weak localisation of optical waves in a disordered medium.

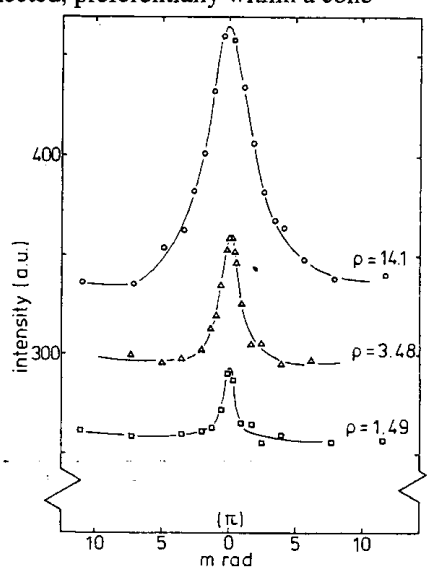

Figure 2.15. Coherent backscattering in a suspension containing 1 μm Latex spheres. ρ is the suspension density.

determined by eq. (2.23) with a total angle

$$\delta_{cone} = 2\delta_{max} \sim \sqrt{\lambda_F / l_e} \qquad (2.35)$$

Note that this expression is formally only "correct" for the 2D case; however it is found to depend only very weakly on dimensionality. We want to describe an optical (=electromagnetic wave) experiment which nicely demonstrates this coherent backscattering.

Figure 2.14 shows the set-up for this experiment (Albeda et.al., Phys. Rev. Lett. 55, 2692-2695 (1985)). Then optical wave is provided by a He-Ne laser. The diffusive medium is realised by dispersing Latex polystyrene spheres of ~ 1 μm diameter in water. The effective elastic mean free path could be varied by changing the the density of the suspension. The laser beam reaches the diffusive cell (which contains the "milky" suspension) via a beam splitter. The beam reflected from the cell is measured by a photo detector PD. The position of the detector can be varied in space, which allows an angular dependent determination of the reflected beam. The results of these measurements are shown in figure 2.14. The three sets of data are for different concentration of the particles in the suspension. The solid curves are fits to a more complete theory, but the typical angle is found to be in very good agreement with our simple eq. (2.23).

2.4 Closing remarks

In this chapter we have discussed a number of classical and one quantum phenomenon that are characteristic for mesoscopic systems in the diffusive regime. Here we want to make one additional remark derived from the quantum phenomenon of weak localisation. As we have shown this results from the complex electron wave interference in the diffusive background. It is of interest to briefly reconsider the magnitude of the effect, as given by eq. (2.28). Apart from the weak (logarithmic) dependence on the ratio of the times for phase breaking and elastic scattering, the typical amplitude in the change of the conductance due to WL amounts to e^2/h, i.e. the conductance quantum. Stated differently, irrespective of the *details* of the distribution of elastic scatterers (i.e., the *microscopic configuration*), the quantum effect on the conductance always is of the *same order of magnitude*. On the other hand, it will be clear that changing the configuration of the scatterers will result in some change in the conductance. Combining these arguments points towards the presumption that *varying the microscopic details of a mesoscopic diffusive medium while maintaining its macroscopic, average properties, leads to variations in the conductance that will be (typically) no larger than the conductance quantum.*

This conclusion can be verified in a much more rigid way, and the important and highly fundamental phenomenon of such fluctuations in the conductance of diffusive systems is very well known in the literature under the name of *Universal Conductance Fluctuations* or *UCF*. The adjective "universal" stresses the role of the conductance quantum in this respect. In addition to Weak Localisation it is the second important quantum phenomenon found in diffusive mesoscopic systems.

General references to the subject

1. "Quantum Transport in Semiconductor Nanostructures" by C.W.J. Beenakker and H. van Houten, in Solid State Physics, ed. H. Ehrenreich & D. Turnbull, Vol 44 (Academic Press Inc., 1991), sections 4, 5, 6 and 7.